Characterization of Nanoscale Carbon-Aluminum Composites (Covetics)

THE DEPARTMENT of MATERIALS SCIENCE AND ENGINEERING

Isaac Mastel, Dr. Jiancun Rao, Dr. Lourdes Salamanca-Riba

UNIVERSITY OF MARYLAND 18 56 MARYLAND ENERGY INNOVATION INSTITUTE

Covetic Preparation[2]

Fabrication

Rods of aluminum 1350 and graphite were placed in a crucible, brought to melting, stirred, then allowed to cool. This was done while a DC current was applied and in an inert atmosphere of argon, which was pumped through the impeller during stirring as well. Processing parameters that were varied and their minimum/maximum values are presented in table 1:

Parameter	Minimum	Maximum
Stir Speed	none	800rpm
Wt% Carbon	0	3
Wt% Copper	0	3
Anneal	none	400°C, 1 hour
Applied Current	none	150A

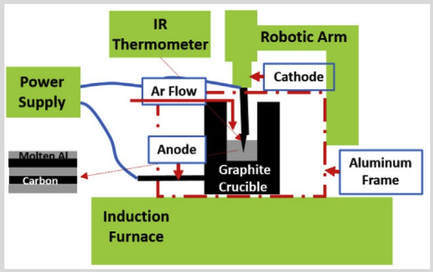

Figure 1: Diagram of covetic sample fabrication [2]

Polishing

Covetic samples were cut into small pieces (~1 cm^2, large variation) and polished starting with 180 grit SiC paper, then AlO polishing papers from 30µm to 0.3µm, until finally being polished with 0.05µm silica suspension on a cotton pad. Water was used to clean any remaining silica from the surface, then it was rinsed with ethanol and dried with compressed air. This process was required to create a perfect enough surface to perform EBSD on the samples.

Figure 2: Polished covetic samples, H-49 (top) and 20210706 (bottom)

Abstract

Metal matrix nanocarbon composites show great promise in the realm of electrical conductivity. Aluminum matrix composites with 1-3 wt% carbon (covetics) are studied here. The increased charge carrier mobility offered by graphene nanoribbons that form during solidification allow the covetic samples to have ~5.6% increased conductivity as compared with the base aluminum alloy [1]. We seek to better understand the role that each processing parameter has on measured electrical conductivity, however first we must understand the relationship between microstructure of the covetics and conductivity. To that end, optical microscopy, electron backscatter diffraction (EBSD), and Raman spectroscopy have been employed, which show graphitic carbon in many of the samples as well as a statistically significant increase in nanoscale carbon crystallite size from the base purchased graphite powder.

Characterization

Optical Microscopy

After polishing, the surface of some samples were etched with Weck's Reagent to see grain boundaries. When this solution didn't give the desired visibility, etchant A (Sigma-Aldrich) was used instead. Grain boundaries were traced in Adobe Photoshop, and ImageJ was then used to analyze grain size.

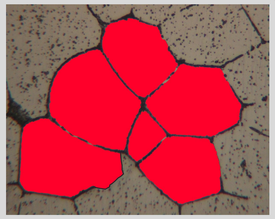

Figure 3: Microscope image showing grains (sample 20190408)

EBSD

EBSD was also used to better understand grain sizes across samples, however the white light images were mainly used instead due to the challenges of properly polishing samples for EBSD. Despite this, EBSD was still able to provide an illustrative example of how the covetic samples' grains compared to that of the base aluminum alloy.

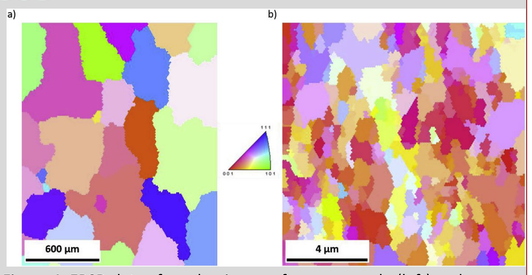

Figure 4: EBSD data of an aluminum reference sample (left) and a covetic sample (right) showing large differences in grain size [2]

Raman

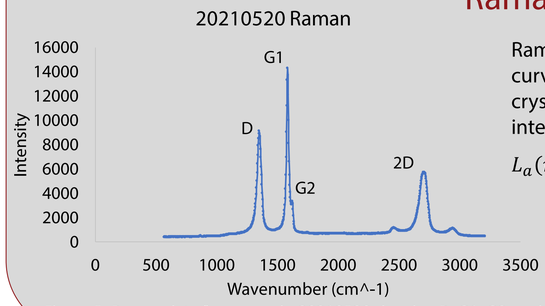

Figure 5: Raman data from sample 20210520 showing D, G1, G2, and 2D peaks

Raman data was collected and Excel was used to fit curves to the D, G1, and G2 peaks. Graphite crystallite size was estimated using the integrated intensities of the peaks according to equation 1 [1]:

$$L_a(nm) = \frac{560}{E_1^4}\left(\frac{I_D}{I_G}\right)^{-1} \qquad \text{(eqn. 1)}$$

Results

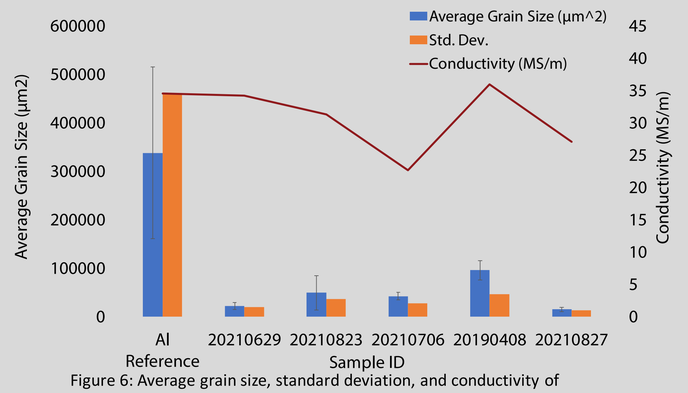

Figure 6: Average grain size, standard deviation, and conductivity of different samples

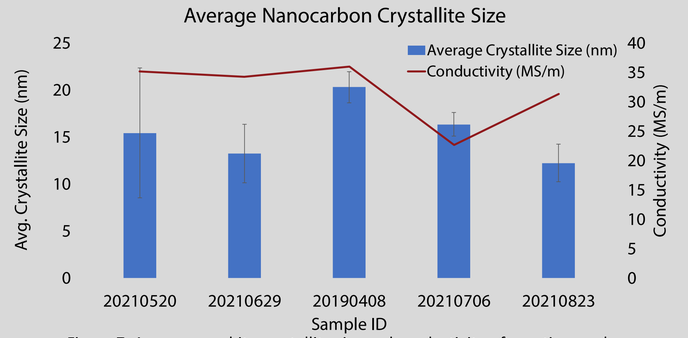

Figure 7: Average graphite crystallite size and conductivity of covetic samples

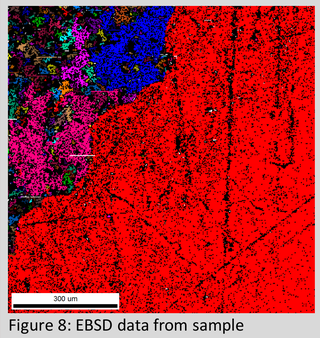

Figure 8: EBSD data from sample 20190408 showing the low misorientation between grains (large red area covering multiple grains)

Conclusion

The large area of red covering multiple grains in the EBSD data shows that covetic samples had less misorientation between grains as compared to the Al reference sample. This was common among the samples. In addition, despite a clear difference in grain size (vs the reference sample) and differences in graphite crystallite size between samples, more investigation is required to correlate these microstructural differences and electrical conductivity.

References/Acknowledgements

[1] Ge, X., Klingshirn, C., Morales, M., Wuttig, M., Rabin, O., Zhang, S., & Salamanca-Riba, L. (2021). Electrical and structural characterization of nano-carbon-aluminum composites fabricated by electro-charging-assisted process. *Carbon*, 115-125. doi:https://doi.org/10.1016/j.carbon.2020.10.063

[2] Ge, X., Klingshirn, C., Wuttig, M., Gaskel, K., Zavalij, P., Liang, Y., . . . Salamanca-Riba, L. (2019). Mechanism studies and fabrication for the incorporation of carbon into Al alloys by the electro-charging assisted process. Carbon, 203-212. doi:https://doi.org/10.1016/j.carbon.2019.04.049

We would like to acknowledge the financial support of NSF Grant DMR2149982, REU/RET Site: Summer Research Experiences in Renewable and Sustainable Energy Technology (ReSET) and the Maryland Energy Innovation Institute (MEI²) and University of Maryland Department of Materials Science and Engineering.

In addition, we would like to acknowledge the guidance and support of Stephen Frazier, Xiaoxiao Ge, and Madeline Morales who grew the samples when they were at UMD, Kenny McAfee who took conductivity measurements, Dr. Karen Gaskell from the Surface Analysis Center, and the UMD Nanocenter for its AIM lab and FabLab

Figure 4: Raman data from sample 20210520 with D, G1, and G2 peaks